

## Antisense Suppression of Pygopus2 Results in Growth Arrest of Epithelial Ovarian Cancer

Cathy M. Popadiuk,<sup>1,2</sup> Jieying Xiong,<sup>1</sup> Malcolm G. Wells,<sup>1</sup> Phillip G. Andrews,<sup>1</sup> Kweku Dankwa,<sup>3</sup> Kensuke Hirasawa,<sup>1</sup> Blue B. Lake,<sup>1</sup> and Kenneth R. Kao<sup>1</sup>

**Abstract Purpose:** The Pygopus proteins are critical elements of the canonical Wnt/ $\beta$ -catenin transcriptional complex. In epithelial ovarian cancer, constitutively active Wnt signaling is restricted to one (endometrioid) tumor subtype. The purpose of this study was to determine the level of expression and growth requirements of human Pygopus2 (hPygo2) protein in epithelial ovarian cancer.

**Experimental Design:** Expression and subcellular localization of hPygo2 was determined in epithelial ovarian cancer cell lines and tumors using Northern blot, immunoblot, and immunofluorescence. Immunohistochemistry was done on 125 archived patient epithelial ovarian cancer tumors representing all epithelial ovarian cancer subtypes. T-cell factor–dependent transcription levels were determined in epithelial ovarian cancer cells using TOPflash/FOPflash *in vivo* assays. Phosphorothioated antisense oligonucleotides were transfected into cell lines and growth assayed by cell counting, anchorage-independent colony formation on soft agar, and xenografting into severe combined immunodeficient mice.

**Results:** All six epithelial ovarian cancer cell lines and 82% of the patient samples overexpressed nuclear hPygo2 compared with control cells and benign disease. Depletion of hPygo2 by antisense oligonucleotides in both Wnt-active (TOV-112D) and Wnt-inactive serous (OVCAR-3, SKOV-3) and clear cell (TOV-21G) carcinoma cell lines halted growth, assessed using tissue culture, anchorage-independent, and xenograft assays.

**Conclusions:** hPygo2 is unexpectedly widely expressed in, and required in the absence of, Wnt signaling for malignant growth of epithelial ovarian cancer, the deadliest gynecologic malignancy. These findings strongly suggest that inhibition of hPygo2 may be of therapeutic benefit for treating this disease.

Deregulation of developmentally important genes in adults can contribute to malignant disease. For instance, the canonical Wnt/ $\beta$ -catenin pathway is normally required for embryonic development and for the controlled proliferation of adult stem cells (1–3) but is frequently abnormally activated in cancer. Determining critical components of this pathway, therefore, is an important means to identify novel therapeutic targets.

In canonical Wnt/ $\beta$ -catenin signaling, binding of the Wnt ligand to its receptor initiates an intracellular signaling cascade resulting in the stabilization of cytoplasmic  $\beta$ -catenin, allowing it to accumulate in the nucleus where it converts the lymphoid enhancer/T-cell factor (LEF)/T-cell factor (TCF)-1 complex from a gene transcriptional repressor into an activator. The *pygopus* genes encode proteins that have been shown to function in this pathway during early embryogenesis as a component of the LEF/TCF-1 complex (4–7). Pygopus is proposed to play a role in the activator function of the complex by acting either as a nuclear “escort” (8) or as a critical link in the complex that recruits the basal transcription machinery (9–11).

Pygopus is likely important for Wnt signaling in cancer cells. For example, transfection of siRNA sequences targeting Pygopus mRNA in established colorectal cancer cell lines resulted in inhibition of TCF/LEF–mediated transcriptional activation of reporter genes (7, 8). However, the levels of reduction of endogenous Pygopus protein were not assessed in these studies. Whether the depletion of Pygopus resulted in phenotypic changes to the malignant cells was also not determined. Indeed, the expression of endogenous Pygopus proteins has yet to be assessed in any malignancy. Understanding of the requirement of Pygopus proteins in cancer, therefore, is far from complete.

In humans, there are two *pygopus* genes, *hPygo1* and *hPygo2*, both of which are presumed to have overlapping, if not

**Authors' Affiliations:** <sup>1</sup>Terry Fox Cancer Research Laboratories, Division of Basic Medical Sciences, and Divisions of <sup>2</sup>Women's Health and <sup>3</sup>Laboratory Medicine, Faculty of Medicine, Memorial University of Newfoundland, St. John's, Newfoundland, Canada

Received 11/8/05; revised 1/19/06; accepted 2/1/06.

**Grant support:** Canadian Institutes of Health Research and Cancer Research Society.

The costs of publication of this article were defrayed in part by the payment of page charges. This article must therefore be hereby marked *advertisement* in accordance with 18 U.S.C. Section 1734 solely to indicate this fact.

**Note:** Supplementary data for this article are available at Clinical Cancer Research Online (<http://clincancerres.aacrjournals.org/>).

B. B. Lake is currently at Mount Sinai Hospital School of Medicine, One Gustave Levy Place, New York, NY 10029-6574.

**Requests for reprints:** Kenneth R. Kao, Terry Fox Cancer Research Laboratories, Division of Basic Medical Sciences, Faculty of Medicine, Memorial University of Newfoundland, 300 Prince Philip Drive, St. John's, NL, Canada A1B 3V6. Phone: 709-777-6860; Fax: 709-777-7391; E-mail: kkao@mun.ca.

©2006 American Association for Cancer Research.  
doi:10.1158/1078-0432.CCR-05-2433



the underlying layer of solidified agarose. Fresh medium was carefully added at 1 week intervals and colonies counted after 30 days.

**Xenograft assays.** SK-OV-3 epithelial ovarian cancer cells were transferred s.c. into severe combined immunodeficient mice (Charles River Laboratories, Saint-Constant, Quebec, Canada) essentially as described (23). Cells were transfected with the antisense oligonucleotides as described above. Four hours after transfection, cells were trypsinized, resuspended in an equal volume of Matrigel at 18°C for a final volume of 0.5 mL, and injected s.c. in mice. Animals were monitored daily for tumor growth and sacrificed after 17 weeks. The maximum tumor length was measured using precision digital calipers (Lee Valley Tools, Ottawa, Canada). Tumors were dissected and weighed using an analytic balance.

## Results

**hPygo2 is overexpressed in epithelial ovarian cancer cell lines.** The expression of hPygo2 in epithelial ovarian cancer cell lines was investigated by Northern blot, immunoblot, and immunocytochemical analyses. We found that hPygo2 mRNA levels were significantly higher in the six cancer cell lines we tested, relative to that of normal surface epithelial cells (Fig. 1A). In addition, whereas hPygo2 protein was found in epithelial ovarian cancer cells, it was barely detectable in the normal primary cultured ovarian surface epithelial cells (Fig. 1B). These observations suggested that overexpression of hPygo2 is a characteristic of epithelial ovarian cancer cell lines.

Previous studies indicated that Pygopus proteins were active in the nuclei of embryonic cells (8). We therefore examined the subcellular localization of endogenous hPygo2 in three different epithelial ovarian cancer cell lines and in a nonmalignant, immortalized ovarian epithelial cell line (iOSE397). Nuclear localization of hPygo2 was confirmed by staining OVCAR-3 cells with a DNA-specific fluorescent dye (Fig. 1C, *Nucl*). Nuclear expression of hPygo2 was consistent in two other malignant lines, TOV21G and TOV112D (Fig. 1D). hPygo2 was also expressed in a perinuclear pattern in the immortalized, nonmalignant control cell line (Fig. 1D, iOSE397). In OVCAR-3 cells (Fig. 1C),  $\beta$ -catenin was localized mainly to the plasma membrane, consistent with previous findings (24).  $\beta$ -Catenin was localized mainly to the plasma membrane in immortalized iOSE397 cells as well (Fig. 1D) and was not detectable in the TOV-21G cells, consistent with previous findings (15–17).  $\beta$ -catenin was, however, expressed at relatively high levels in the cytoplasm and nuclei of TOV-112D (endometrioid) cells, as expected, because this cell line has high levels of constitutive canonical Wnt signaling (15). These observations suggest that although  $\beta$ -catenin has variable subcellular expression, hPygo2 is consistently expressed in nuclei of epithelial ovarian cancer cells. Thus, hPygo2 and  $\beta$ -catenin do not necessarily colocalize to nuclei in epithelial ovarian cancer cell lines.

**Nuclear localization of hPygo2 in epithelial ovarian cancer.** To determine the prevalence of hPygo2 expression in epithelial ovarian cancer disease, we analyzed the *in situ* localization of hPygo2 protein in 125 tumors from archived surgical samples. We semiquantitatively assessed expression based on intensity and percentage of tumor cells stained in both the cytoplasm and nuclei (Fig. 1E). All epithelial ovarian cancer histologic tumor subtypes, including serous, mucinous, clear cell, endometrioid, and undifferentiated were represented in our sample set, but the majority, as expected,

were of the serous subtype (25, 26). The tumor subtypes and distribution of level and localization (either nuclear or cytoplasmic) of hPygo2 staining for each subtype is displayed in Table 1.

hPygo2 was undetectable or very weakly expressed in the nuclei of nonmalignant or benign ovarian tumors, such as cystadenomas (Fig. 1E, –). On the other hand, as shown in Table 1 (“total” column for nuclear staining), 82% of the tumors with a pathologic diagnosis consistent with malignant epithelial ovarian cancer had moderate (“++”, 52%) to strong (“+++”, 30%) nuclear accumulation of hPygo2 protein. This abnormal accumulation of hPygo2 protein was observed in tumor cells but not in the surrounding stromal cells (Fig. 1E and F, *red arrows*). In addition, hPygo2 was found in the nuclei of tumors representing all of the epithelial ovarian cancer histologic subtypes (Table 1). These observations are consistent with a role for hPygo2 as a nuclear protein in malignant epithelial ovarian cancer disease.

$\beta$ -Catenin subcellular localization was compared with nuclear hPygo2 staining in adjacent sections from 87 of the 125 tumor specimens from the patients diagnosed with malignant epithelial ovarian cancer collected above (Fig. 1F; Supplementary Table S2). Eight (9.2%) tumors stained positive for nuclear  $\beta$ -catenin, a result similar to previous findings (24). Eighty-four (97%) tumors stained positive for nuclear hPygo2, eight (9.2%) of which simultaneously stained for nuclear  $\beta$ -catenin. None of the tumors stained exclusively for nuclear  $\beta$ -catenin and only one tumor did not stain for either protein. These observations indicated that relative to  $\beta$ -catenin, hPygo2 is highly expressed in the nuclei of epithelial ovarian cancer cells. Thus, as with the cell lines, hPygo2 and  $\beta$ -catenin do not necessarily colocalize in epithelial ovarian cancer tumors.

**hPygo2 knockdown causes growth arrest of Wnt-inactive epithelial ovarian cancer cell lines.** The observation that hPygo2 was more frequently expressed in nuclei than  $\beta$ -catenin in epithelial ovarian cancer cell lines and in tumors with diverse subtypes raised the hypothesis that it has activity in cancer cells that are not active in canonical Wnt signaling. We confirmed and extended the findings of others (16, 24) that TCF-dependent transcriptional activity was absent in two serous carcinoma-derived cell lines (SKOV-3 and OVCAR-3) and one clear cell carcinoma line (TOV-21G) but, in comparison, significantly active ( $P < 0.00001$ ,  $n = 9$ ) in cell lines of endometrioid (TOV112D) origin (Fig. 1G).

The requirement of hPygo2 in epithelial ovarian cancer cells was determined by transfecting phosphorothioated antisense oligonucleotides to knock down hPygo2 mRNA and its protein, initially in the serous tumor-derived epithelial ovarian cancer cell lines OVCAR-3 and SKOV-3. Both hPygo2 mRNA and protein levels were significantly reduced by an antisense oligonucleotide, hPy-ON5, without affecting the expression of hPygo1 RNA or  $\beta$ -catenin protein (Fig. 2A). The sequence of hPyOn5 is complementary to nucleotides at positions 634 to 652 (from the start of translation), within the coding region of hPygo2 mRNA. Of the two cell lines tested, the antisense oligonucleotide reduced endogenous hPygo2 protein by ~40% in SK-OV-3 cells and 30% in OVCAR-3 cells when compared with controls (Fig. 2A), which included untransfected cells (*Cont.*), cells treated only with transfection reagents (*Reag.*), and cells transfected with the mismatched control oligo. To confirm the specificity of the antisense knockdown, we

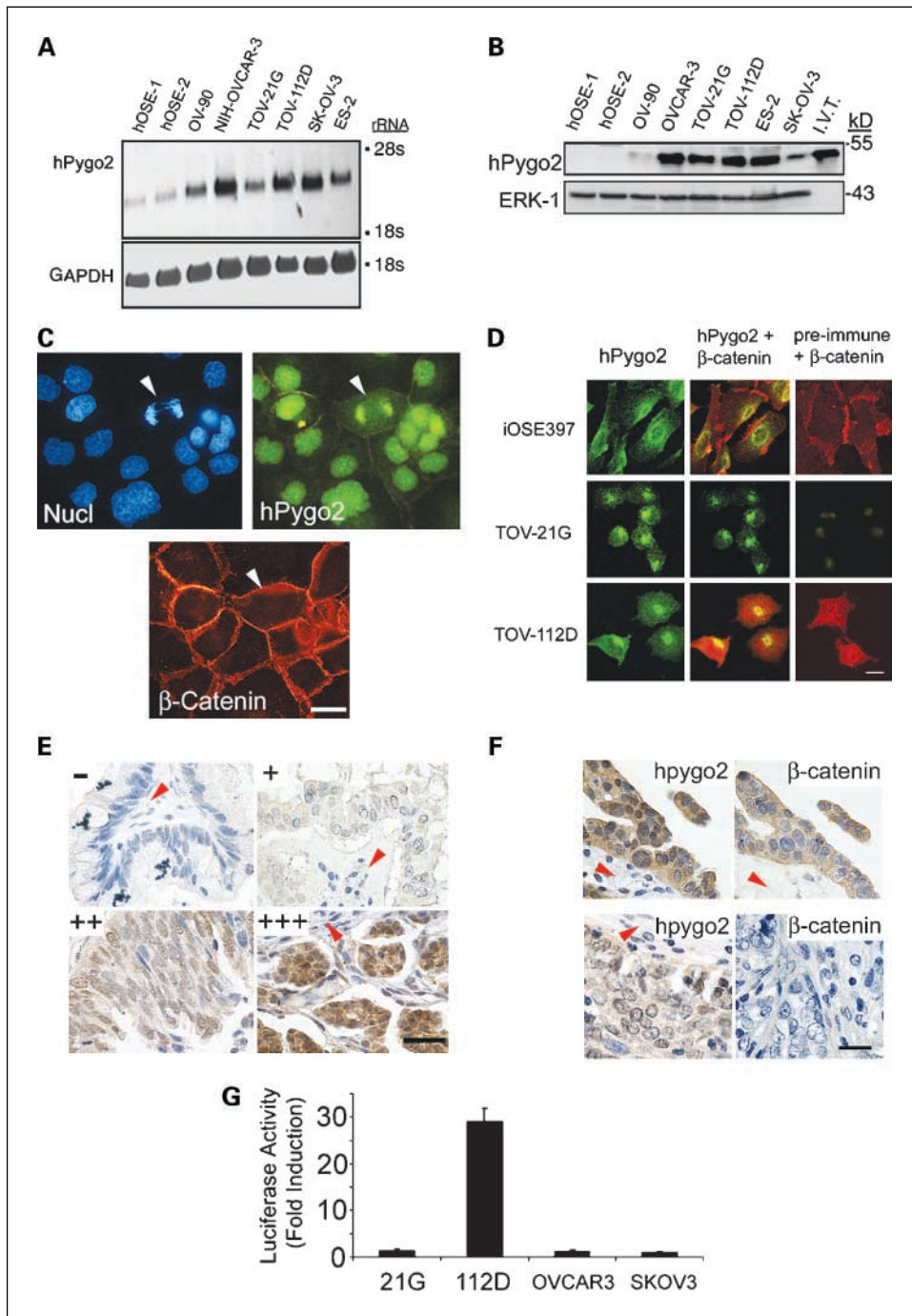


**Fig. 1.** Expression analyses of hPygo2 and TCF-dependent transcription in epithelial ovarian cancer tumors and cell lines. **A**, expression of hPygo2 RNA in epithelial ovarian cancer cell lines using Northern analysis. Positions of the 28S and 18S rRNA are shown. Glyceraldehyde-3-phosphate dehydrogenase (*GAPDH*) was used as a loading control. **B**, expression of hPygo2 protein in epithelial ovarian cancer and human ovarian surface epithelial cell lines using immunoblots. *In vitro* synthesized hPygo2 (*hVT*) was used as a positive control. ERK-1 is used as a loading control. Molecular weight is expressed in kilodaltons (*kD*). **C**, OVCAR-3 cells were stained simultaneously with nuclear-specific Hoechst 33342 dye (*Nucl*), hPygo2 antisera (*hPygo2*) detected with fluorescein-conjugated secondary antibodies, and  $\beta$ -catenin monoclonal antibodies detected with Texas red-conjugated secondary antibodies ( *$\beta$ -catenin*) and viewed under a fluorescence microscope. Arrowhead, position of an anaphase stage cell. Bar, 5  $\mu$ m. **D**, immortalized epithelial ovarian cells (*IOSE397*) and two epithelial ovarian cancer cell lines (*TOV-21G* and *TOV-112D*) were processed for confocal immunofluorescent detection of hPygo2 (*green fluorescence*) and  $\beta$ -catenin (*red fluorescence*). Left column, expression of hPygo2 alone; middle column, additional expression of  $\beta$ -catenin; right columns, expression of  $\beta$ -catenin alone. Bar, 20  $\mu$ m. **E**, hPygo2 protein expression in tumors was graded according to intensity and frequency of tumor cell nuclei staining (*brown*) with hPygo2 antisera in relation to background staining of surrounding stromal tissue (*red arrows*). All nuclei were stained in blue with hematoxylin. Some visible features of malignant cells used in the analysis include larger than normal nuclei, disorganized cellular arrangement, and invasion of the stroma. Nonmalignant ovarian epithelial adenomas are negative (-) for hPygo2. Staining of malignant tumors ranged from weak (+, light staining or <60% nuclei stained) to moderate (++, intermediate intensity staining, 80% nuclei stained) to strong (+++, intense staining with >90% nuclei stained). Bar, 30  $\mu$ m. **F**, examples of hPygo2 and  $\beta$ -catenin expression in adjacent tumor sections. Top pair, strong nuclear staining of hPygo2 in a tumor coincident with weak nuclear and moderate cytoplasmic  $\beta$ -catenin staining. Bottom pair, coincident moderate hPygo2 nuclear staining and negative  $\beta$ -catenin staining. Bar, 22  $\mu$ m. **G**, activation of TCF-dependent transcription in TOV112D endometrioid adenocarcinoma cells, TOV21G clear cell carcinoma, and SKOV-3 and OVCAR-3 serous carcinoma cells. Columns, means of three independent experiments repeated in triplicate; bars, SD.

**Table 1.** Frequency distribution of histologic tumor subtypes (percentages in parentheses) according to level (– to +++) of nuclear and cytoplasmic hPygo2 staining

		Tumor subtype						Total
		Benign	Mucinous	Endometrioid	Serous	Clear cell	Undifferentiated	
Nuclear	–	7 (100)	3 (21)	0	2 (2)	0	0	12 (10)
	+	0	1 (7)	1 (12)	8 (9)	0	0	10 (8)
	++	0	7 (50)	5 (63)	46 (53)	4 (80)	3 (75)	65 (52)
	+++	0	3 (21)	2 (25)	31 (36)	1 (20)	1 (25)	38 (30)
	Total	7 (100)	14 (100)	8 (100)	87 (100)	5 (100)	4 (100)	125 (100)
Cytoplasmic	–	5 (72)	4 (29)	0	12 (14)	0	0	21 (17)
	+	0	6 (43)	5 (63)	53 (61)	5 (100)	1 (25)	70 (56)
	++	1 (14)	3 (21)	3	21 (24)	0	2 (50)	30 (24)
	+++	1 (14)	1 (7)	0 (37)	1 (1)	0	1 (25)	4 (3)
	Total	7 (100)	14 (100)	8 (100)	87 (100)	5 (100)	4 (100)	125 (100)

repeated the above experiments using an antisense oligonucleotide (hPy-ON8) targeting the 3' untranslated region of *hPygo2* mRNA, spanning nucleotides 1,644 to 1,662 from the start of translation. The levels of hPygo2 protein reduction using this antisense oligonucleotide were similar to the levels when we used hPy-ON5 (Fig. 2B).

The two cell lines we initially tested for knockdown of hPygo2 by antisense oligonucleotides underwent significant reduction in cell number for SK-OV-3 cells at 48 hours ( $P = 0.0003$ ,  $n = 12$ ) and 72 hours ( $P = 0.002$ ,  $n = 12$ ) posttransfection and for OVCAR-3 cells 48 hours ( $P = 0.001$ ,  $n = 12$ ) and 72 hours ( $P = 0.0005$ ,  $n = 12$ ) posttransfection using hPy-ON5 (Fig. 3A) compared with cells transfected with the mismatched control oligonucleotide. Similar results were obtained using hPy-ON8 (Fig. 3B, all  $P < 0.005$ ,  $n = 12$ ).

**Antisense knockdown of hPygo2 is reversible.** We next attempted to rescue the effect of the antisense treatment by cotransfection of hPygo2 to further confirm that the knockdown we observed was due to specific reduction of wild-type hPygo2 protein. To restore hPygo2 protein expression reduced by the antisense treatment, hPy-ON8 antisense oligonucleotides were cotransfected with an expression vector (pCS2+) containing only the coding region of hPygo2. Cotransfection of this plasmid with hPy-ON8 antisense oligonucleotides that target noncoding sequences restored the levels of hPygo2 protein close to control levels compared with cells cotransfected with empty vector and hPy-ON8, which showed significant hPygo2 protein reduction (Fig. 3C).

The significant reduction in cell numbers by treatment with hPy-ON8 (Fig. 3D) at 48 hours ( $P = 0.0004$ ,  $n = 9$ ) and 72 hours ( $P = 0.01$ ,  $n = 9$ ) was restored to levels of the controls (empty vector plus mismatched control oligo) at 48 hours ( $P = 0.94$ ,  $n = 9$ ) and 72 hours ( $P = 0.96$ ,  $n = 9$ ) by exogenously introducing the coding region sequences of *hPygo2* (Fig. 3D). It is likely, therefore, that the effects on cell numbers by transfection of hPy-ON8 were specific to reduction of endogenous hPygo2 RNA and hPygo2 protein as opposed to off-target effects. These results indicate that hPygo2-specific antisense sequences inhibit epithelial ovarian cancer cell growth by specifically reducing endogenous hPygo2 protein levels.

**hPygo2 is required for growth of a  $\beta$ -catenin-deficient cell line.** The growth requirements for hPygo2 in SKOV-3 and

OVCAR-3 cells, both of which are derived from serous tumors, suggested that hPygo2 functions in cells not active in Wnt signaling. Unlike endometrioid cells, these cell lines do not seem to constitutively activate TCF/LEF-1-dependent transcription but it is possible that Wnt activation occurs transiently so the detection of nuclear  $\beta$ -catenin, for instance, would be easily missed in these cells. To confirm that hPygo2 has activity in non-Wnt active epithelial ovarian cancer cells, we determined the effect of depleting hpygo2 in the clear cell tumor-derived TOV-21G cell line, which does not express  $\beta$ -catenin and in which TCF-dependent transcription is imperceptible, if not absent (Fig. 1G). As a comparison, we determined the effect of knocking down hPygo2 in TOV-112D cell lines, which show

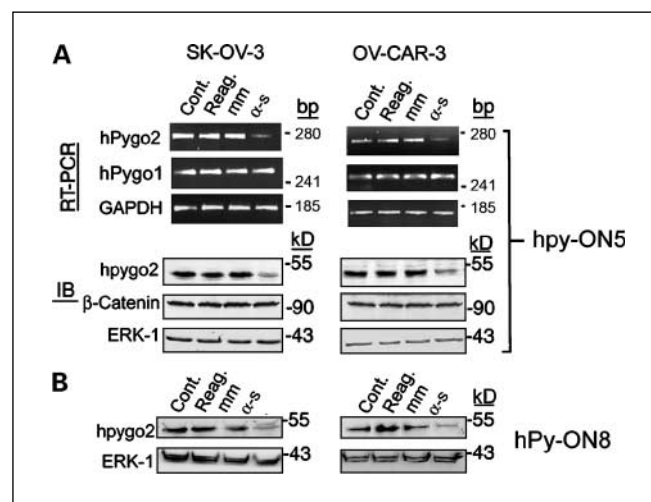


**Fig. 2.** Knockdown of hPygo2 protein in SK-OV-3 and OVCAR-3 epithelial ovarian cancer cells by antisense oligonucleotides. **A**, cells were transfected with the hPygo2 antisense oligonucleotide, hPy-ON5 ( $\alpha$ -s), or mismatched control (*mm*) oligonucleotides and compared with untransfected (*Cont.*) or mock-transfected (*Reag.*) cells and assayed by reverse transcription-PCR (RT-PCR) and immunoblotting (IB) for hPygo2, hPygo1, and  $\beta$ -catenin expression. Glyceraldehyde-3-phosphate dehydrogenase expression was used as a loading control for reverse transcription-PCR and ERK-1 for immunoblots. Amplification product sizes are expressed in bp. **B**, cells were transfected with the hPygo2 antisense oligonucleotide, hPy-ON8, or mismatched control oligonucleotides and compared with untransfected or mock-transfected cells and assayed by immunoblot with ERK-1 as a loading control.

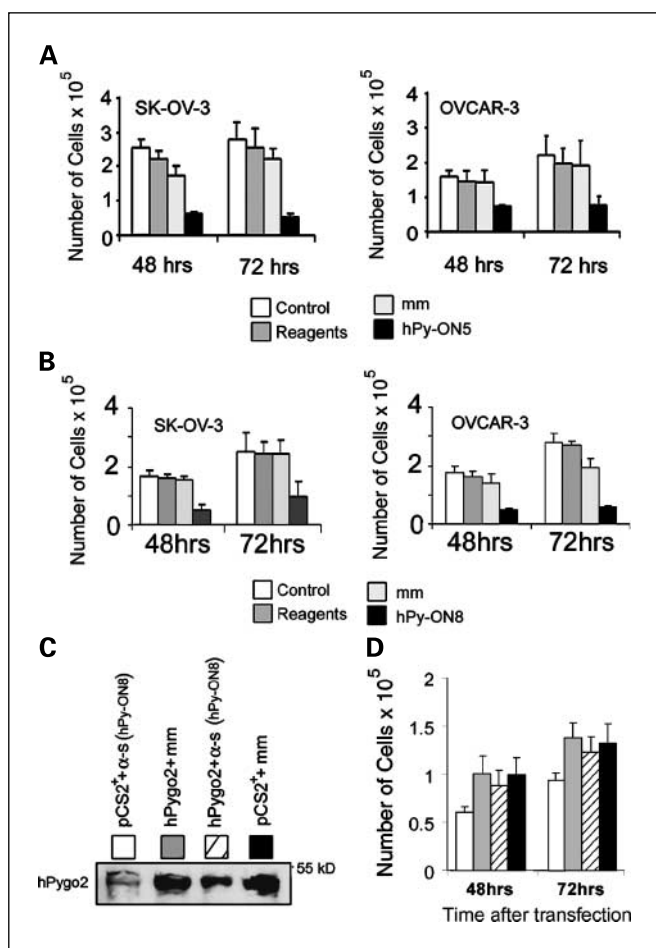


**Fig. 3.** Knockdown of hPygo2 reduces epithelial ovarian cancer cell numbers. **A**, results of growth assays of SK-OV-3 and OVCAR-3 cells transfected with the hPy-ON5 antisense oligonucleotide and mismatched control oligonucleotides 48 and 72 hours after transfection. Columns, mean; bars, SD. **B**, results of growth assays of SK-OV-3 and OVCAR-3 cells transfected with the hPy-ON8 antisense oligonucleotide and mismatched control oligonucleotides 48 and 72 hours after transfection. Columns, mean; bars, SD. **C**, hPygo2 cotransfection restores protein levels in cells depleted of hPygo2 by the hPy-ON8 antisense oligonucleotide ( $\alpha$ -s). SKOV-3 cells were transfected with the hPy-ON8 antisense oligonucleotide (*hPy-ON8*), which targets 3' untranslated sequences of hPygo2 or the mismatched control oligonucleotide together with either an expression plasmid vector containing hPygo2 coding sequence (*hPygo2*) or empty vector (*pCS2+*). Transfected cells were assayed for expression of hPygo2 using Western (immunoblot) analysis 48 hours after transfection. Equal amounts of total protein, as determined by measuring absorbance, were loaded for each sample. **D**, exogenous hPygo2 rescues cell number reduction caused by depletion of endogenous hPygo2. Columns, mean; bars, SD. SKOV-3 epithelial ovarian cancer cells were transfected with antisense oligonucleotides and the numbers of cells were counted (*Yaxis*) 48 and 72 hours posttransfection. Histograms, data corresponding to the treatments shown in (C).

constitutive activation of Wnt signaling (Fig. 1G). We also confirmed the lack of association of hPygo2 with  $\beta$ -catenin in the TOV-21G cell line compared with the TOV112D line using coimmunoprecipitation (data not shown).

Transfection of anti- $\beta$ -catenin antisense oligonucleotides caused close to 60% reduction in endogenous  $\beta$ -catenin protein in TOV-112D cells, whereas transfection of hPygo2 antisense oligonucleotides (hPy-ON8) caused ~50% reduction in hPygo2 levels in both TOV-112D (Fig. 4A) cells and TOV-21G cells (Fig. 4A). The anti- $\beta$ -catenin antisense oligonucleotides did not have an effect on TOV-21G cell growth (Fig. 4B, right), as expected, as these cells do not

express  $\beta$ -catenin (Figs. 1D and 4A). There was, on the other hand, a ~3-fold reduction in cell number at 48 hours ( $P = 0.00002$ ,  $n = 12$ ) and 72 hours ( $P = 0.00004$ ,  $n = 12$ ) after transfection of anti- $\beta$ -catenin antisense oligonucleotides into TOV-112D cells (Fig. 4B). hPygo2 antisense oligonucleotides caused significant growth inhibition of TOV-112D cells (Fig. 4B) after 48 hours ( $P = 0.00001$ ,  $n = 12$ ) and 72 hours ( $P = 0.00001$ ,  $n = 12$ ) and TOV-21G cells (Fig. 4B) after 48 hours ( $P = 0.0001$ ,  $n = 12$ ) and 72 hours ( $P = 0.003$ ,  $n = 12$ ) when compared with the mock-transfected and mismatched control-transfected cells. These results indicated that hPygo2 is required for growth of both constitutively Wnt-active and Wnt-inactive ( $\beta$ -catenin deficient) cell lines.

*hPygo2 is required for anchorage-independent growth and growth in severe combined immunodeficient mice.* We next tested the ability for transfection of antisense oligonucleotides to reduce anchorage-independent growth. hPy-ON5 and hPy-ON8 antisense oligonucleotides (50 nmol/L each) were pooled for transfection. In three separate experiments reproduced in triplicate, there was a significant decrease in the size (Fig. 5A) and number (Fig. 5B,  $P < 0.00001$ ,  $n = 9$ ) of colonies grown in soft agar formed by SK-OV-3 cells transfected with the pooled hPygo2 antisense oligonucleotides, compared with those transfected with the mismatched control oligo.

Our *in vitro* growth inhibition findings were complemented with *in vivo* growth assays to determine whether the *in vivo* culture environment might reverse the initial effects of hPygo2 antisense oligonucleotides. hPygo2 antisense oligonucleotides or mismatched control oligos were transiently transfected into SK-OV-3 cells and then implanted s.c. into severe combined immunodeficient mice. Measurable tumors appeared 11 weeks after transfection in the mice implanted with the control cells (Fig. 5C), whereas mice implanted with

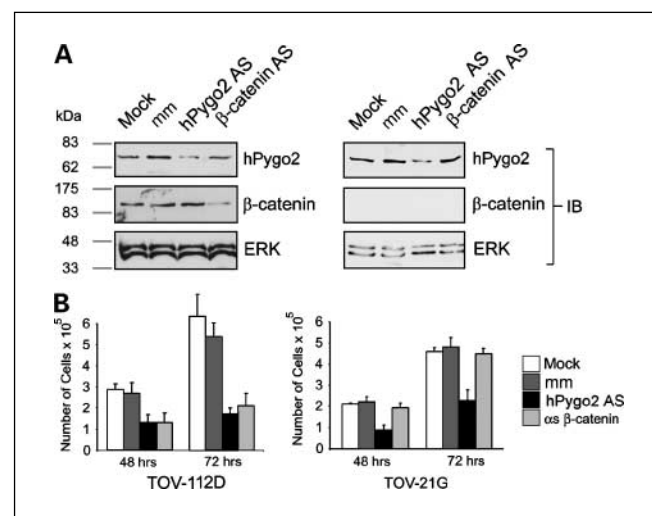


**Fig. 4.** hPygo2 is required for growth of both Wnt-constitutive and Wnt-inactive ( $\beta$ -catenin defective) cell lines. **A**, TOV112D and TOV21G cells were untransfected (*Mock*) or transfected with antisense hPygo2 (*hPygo2 AS*),  $\beta$ -catenin ( *$\beta$ -catenin AS*), or mismatched control oligonucleotides and assayed for knockdown of endogenous protein by immunoblotting using antibodies against hPygo2,  $\beta$ -catenin, and ERK as a loading control. **B**, number of cells was determined at 48 and 72 hours after transfection. Columns, mean; bars, SE.

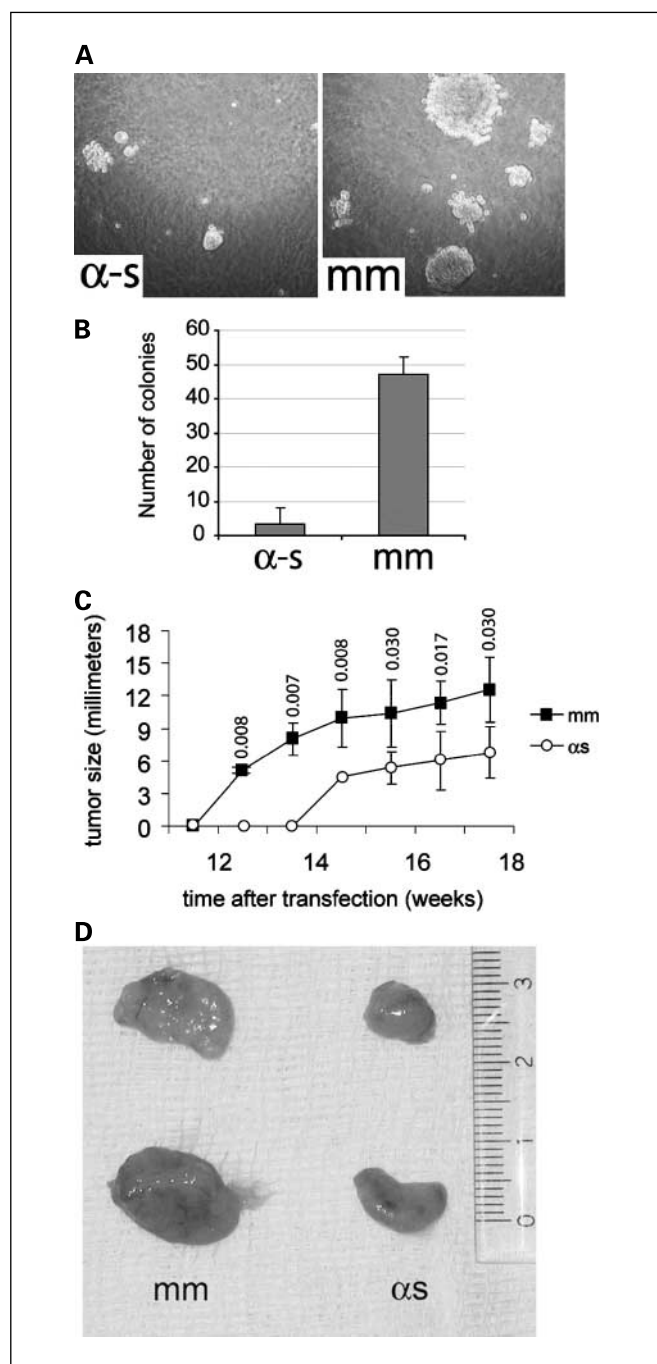


**Fig. 5.** Loss of anchorage-independent growth and growth *in vivo* by antisense hPygo2. *A*, SK-OV-3 cells were transfected with a pooled mixture of hPy-ON5 and hPy-ON8 antisense oligonucleotides and assayed for growth in soft agar. Note the reduction in size of colonies resulting from antisense transfection. *B*, colony numbers of cells transfected with hPygo2 antisense oligonucleotides or the mismatched control recorded 30 days after transfection. *C*, tumors from SK-OV-3 cells transfected with hPygo2 antisense oligonucleotide are growth retarded relative to those from cells transfected with mismatched control oligos (*P* values shown over sample points). *D*, examples of xenografted tumors dissected from animals sacrificed 18 weeks after transfection.

hPygo2 antisense oligonucleotide-treated cells developed tumors after 14 weeks. In all cases, antisense oligonucleotide-transfected cells formed smaller tumors than mismatched control transfected cells throughout the measurable

growth period (Fig. 5C,  $P < 0.03$ ,  $n = 3$ ). After 18 weeks, there was a visible difference (Fig. 5D) in tumor mass ( $P = 0.002$ ,  $n = 3$ ) between mice implanted with cells transfected with hPygo2 antisense oligonucleotides (0.21 g) and those implanted with cells transfected with the mismatched control oligos (0.62 g). These results indicated that *in vivo* culture of hPygo2-transfected cells does not reverse the effect of growth inhibition by antisense hPygo2 antisense oligonucleotides.

## Discussion

Our severe combined immunodeficient mice xenograft assays indicate that the *in vivo* microenvironment does not reduce the effect of depletion of hPygo2 by antisense oligonucleotides. We note, however, that there was not a complete elimination of colony growth or tumor formation and the growth differences between control and hPygo2 antisense oligonucleotide-transfected tumors in the xenograft *in vivo* assay seem to persist many weeks after the initial transfection event. This long-lasting effect would not be expected using the single transient transfection method. We suggest, however, that the immediate effect of knockdown of hPygo2 in cells may be permanent and that the formation of smaller tumors in hPygo2-transfected cells compared with control transfected cells is likely due to a small number of cells that escaped transient transfection. Thus, the effect we observed was equivalent to a smaller seeding of the initial tumor cells. Although we did not achieve full elimination of tumors by transient transfection, our findings necessarily provide the initial results upon which to base more advanced preclinical studies to assess other effects of continuous treatment.

There is much evidence that the canonical Wnt pathway does not likely play a role in epithelial ovarian cancer tumors that are not of endometrioid origin (14, 27, 28). Our results were consistent with this established observation. Because of its previously described dedicated role in canonical Wnt signaling, however, it would not be expected that hPygo2 would play a significant role in this malignancy. We are compelled to hypothesize, therefore, that Pygopus may have functions outside of Wnt signaling, or its constitutive localization to the nuclei of epithelial ovarian cancer cells is sufficient to activate downstream effectors of Wnt signaling in the absence of upstream signaling components.

Other components of the Wnt pathway, such as  $\beta$ -catenin, axin, and APC, are engaged in critical cellular functions apart from canonical signaling (29, 30). We previously showed that mutant Pygopus2 with a deletion of the domain that interacts with the TCF/LEF complex could activate genes associated with vertebrate embryonic nervous system formation (19), suggesting that Pygopus might have undescribed functions. Likewise, our present observations that hPygo2 was expressed in and required for growth of (Wnt inactive) serous and clear cell tumor lines suggests either that overexpressed hPygo2 can function as a downstream effector of the canonical Wnt pathway without interaction with the  $\beta$ -catenin complex, or that it has additional cellular roles. It is equally feasible that hPygo2 may interact with other transcriptional complexes, a possibility we are investigating.

The necessity to identify novel markers and therapeutic targets for epithelial ovarian cancer has provided strong

impetus to search for genes that are important for this disease (31). A variety of mRNAs are now being used as targets for antisense therapy in early phase clinical trials (32), including p53 (33), survivin (34), raf-1 (35), X-linked inhibitor of apoptosis protein (36), and telomerase (37, 38). The overexpression of hPygo2 in epithelial ovarian cancer cell lines and tumors relative to normal epithelia and its requirement for growth strongly suggest that it too is important in epithelial

ovarian cancer and can be added to the growing armamentarium of therapeutic targets.

## Acknowledgments

We thank Nelly Auersperg for access to the Canadian Ovarian Tissue Bank; Al Pater for laboratory space and equipment; Patti McCarthy, Judy Foote, and the late Desmond Robb for help with histopathology; and Garry Chernenko and Yuen-Yee Ho for technical assistance.

## References

- Reya T, Clevers H. Wnt signalling in stem cells and cancer. *Nature* 2005;434:843–50.
- Pinto D, Clevers H. Wnt, stem cells and cancer in the intestine. *Biol Cell* 2005;97:185–96.
- Bienz M.  $\beta$ -Catenin: a pivot between cell adhesion and Wnt signalling. *Curr Biol* 2005;15:R64–7.
- Belenkaya TY, Han C, Standley HJ, et al. Pygopus encodes a nuclear protein essential for wingless/Wnt signaling. *Development* 2002;129:4089–101.
- Kramps T, Peter O, Brunner E, et al. Wnt/wingless signaling requires BCL9/legless-mediated recruitment of pygopus to the nuclear  $\beta$ -catenin-TCF complex. *Cell* 2002;109:47–60.
- Parker DS, Jemison J, Cadigan KM. Pygopus, a nuclear PHD-finger protein required for Wingless signaling in *Drosophila*. *Development* 2002;129:2565–76.
- Thompson B, Townsley F, Rosin-Arbesfeld R, et al. A new nuclear component of the Wnt signalling pathway. *Nat Cell Biol* 2002;4:367–73.
- Townsley FM, Cliffe A, Bienz M. Pygopus and Legless target Armadillo/ $\beta$ -catenin to the nucleus to enable its transcriptional co-activator function. *Nat Cell Biol* 2004;6:626–33.
- Hoffmans R, Basler K. Identification and *in vivo* role of the Armadillo-Legless interaction. *Development* 2004;131:4393–400.
- Hoffmans R, Stadel R, Basler K. Pygopus and legless provide essential transcriptional coactivator functions to armadillo/ $\beta$ -catenin. *Curr Biol* 2005;15:1207–11.
- Townsley FM, Thompson B, Bienz M. Pygopus residues required for its binding to legless are critical for transcription and development. *J Biol Chem* 2004;279:5177–83.
- Verma UN, Surabhi RM, Schmaltieg A, et al. Small interfering RNAs directed against  $\beta$ -catenin inhibit the *in vitro* and *in vivo* growth of colon cancer cells. *Clin Cancer Res* 2003;9:1291–300.
- Li Y, Welm B, Podsypanina K, et al. Evidence that transgenes encoding components of the Wnt signaling pathway preferentially induce mammary cancers from progenitor cells. *Proc Natl Acad Sci U S A* 2003;100:15853–8.
- Kildal W, Risberg B, Abeler VM, et al.  $\beta$ -catenin expression, DNA ploidy and clinicopathological features in ovarian cancer: a study in 253 patients. *Eur J Cancer* 2005;41:1127–34.
- Palacios J, Gamallo C. Mutations in the  $\beta$ -catenin gene (CTNNB1) in endometrioid ovarian carcinomas. *Cancer Res* 1998;58:1344–7.
- Wu R, Zhai Y, Fearon ER, et al. Diverse mechanisms of  $\beta$ -catenin deregulation in ovarian endometrioid adenocarcinomas. *Cancer Res* 2001;61:8247–55.
- Zhai Y, Wu R, Schwartz DR, et al. Role of  $\beta$ -catenin/T-cell factor-regulated genes in ovarian endometrioid adenocarcinomas. *Am J Pathol* 2002;160:1229–38.
- Auersperg N, Siemens CH, Myrdal SE. Human ovarian surface epithelium in primary culture. *In Vitro* 1984;20:743–55.
- Lake BB, Kao KR. Pygopus is required for embryonic brain patterning in *Xenopus*. *Dev Biol* 2003;261:132–48.
- Ju ST, Panka DJ, Cui H, et al. Fas(CD95)/FasL interactions required for programmed cell death after T-cell activation. *Nature* 1995;373:444–8.
- Reynolds JN, Prasad A, Gillespie LL, et al. Developmental expression of functional GABAA receptors containing the  $\gamma$ 2 subunit in neurons derived from embryonal carcinoma (P19) cells. *Mol Brain Res* 1996;35:11–8.
- Rorke S, Murphy, S, Khalifa, M, et al. Prognostic significance of BAG-1 expression in nonsmall cell lung cancer. *Int J Cancer* 2001;95:317–22.
- Elkas JC, Baldwin RL, Pegram M, et al. A human ovarian carcinoma murine xenograft model useful for preclinical trials. *Gynecol Oncol* 2002;87:200–6.
- Lee CM, Shvartsman H, Deavers MT, et al.  $\beta$ -catenin nuclear localization is associated with grade in ovarian serous carcinoma. *Gynecol Oncol* 2003;88:363–8.
- Bell DA. Origins and molecular pathology of ovarian cancer. *Mod Pathol* 2005;18 Suppl 2:S19–32.
- Seidman JD, Kurman RJ. Pathology of ovarian carcinoma. *Hematol Oncol Clin North Am* 2003;17:909–25, vii.
- Faleiro-Rodrigues C, Macedo-Pinto I, Pereira D, et al. Loss of  $\beta$ -catenin is associated with poor survival in ovarian carcinomas. *Int J Gynecol Pathol* 2004;23:337–46.
- Faleiro-Rodrigues C, Macedo-Pinto IM, Maia SS, et al. Biological relevance of E-cadherin-catenin complex proteins in primary epithelial ovarian tumors. *Gynecol Obstet Invest* 2005;60:75–83.
- Bienz M. The subcellular destinations of APC proteins. *Nat Rev Mol Cell Biol* 2002;3:328–38.
- Ciani L, Krylova O, Smalley MJ, et al. A divergent canonical WNT-signaling pathway regulates microtubule dynamics: dishevelled signals locally to stabilize microtubules. *J Cell Biol* 2004;164:243–53.
- See HT, Kavanagh JJ, Hu W, Bast RC. Targeted therapy for epithelial ovarian cancer: current status and future prospects. *Int J Gynecol Cancer* 2003;13:701–34.
- Gleave ME, Monia BP. Antisense therapy for cancer. *Nat Rev Cancer* 2005;5:468–79.
- Killing JS, Squatrito RC, Connor JP, et al. p53 gene mutation analysis and antisense-mediated growth inhibition of human ovarian carcinoma cell lines. *Gynecol Oncol* 1996;60:72–80.
- Ma X, Wang S, Zhou J, et al. Induction of apoptosis in human ovarian epithelial cancer cells by antisurvivin oligonucleotides. *Oncol Rep* 2005;14:275–9.
- Mullen P, McPhillips F, MacLeod K, et al. Antisense oligonucleotide targeting of Raf-1: importance of raf-1 mRNA expression levels and raf-1-dependent signaling in determining growth response in ovarian cancer. *Clin Cancer Res* 2004;10:2100–8.
- Li J, Sasaki H, Sheng YL, et al. Apoptosis and chemoresistance in human ovarian cancer: is Xiap a determinant? *Biol Signals Recept* 2000;9:122–30.
- Yuan B, Mi R. [Antisense oligodeoxynucleotides of human telomerase catalytic sub-unit inhibits telomerase activity and proliferation in SKOV3 and COC1]. *Zhonghua Fu Chan Ke Za Zhi* 2002;37:198–201.
- Kushner DM, Paranjape JM, Bandyopadhyay B, et al. 2-5A antisense directed against telomerase RNA produces apoptosis in ovarian cancer cells. *Gynecol Oncol* 2000;76:183–92.



# Clinical Cancer Research

## Antisense Suppression of Pygopus2 Results in Growth Arrest of Epithelial Ovarian Cancer

Cathy M. Popadiuk, Jieying Xiong, Malcolm G. Wells, et al.

*Clin Cancer Res* 2006;12:2216-2223.

**Updated version** Access the most recent version of this article at:  
<http://clincancerres.aacrjournals.org/content/12/7/2216>

**Cited articles** This article cites 38 articles, 10 of which you can access for free at:  
<http://clincancerres.aacrjournals.org/content/12/7/2216.full#ref-list-1>

**Citing articles** This article has been cited by 16 HighWire-hosted articles. Access the articles at:  
<http://clincancerres.aacrjournals.org/content/12/7/2216.full#related-urls>

**E-mail alerts** [Sign up to receive free email-alerts](#) related to this article or journal.

**Reprints and Subscriptions** To order reprints of this article or to subscribe to the journal, contact the AACR Publications Department at [pubs@aacr.org](mailto:pubs@aacr.org).

**Permissions** To request permission to re-use all or part of this article, use this link  
<http://clincancerres.aacrjournals.org/content/12/7/2216>.  
Click on "Request Permissions" which will take you to the Copyright Clearance Center's (CCC) Rightslink site.